# High Frame Rate 2D and 3D Imaging with a Curved or Cylindrical Array

Hu Peng and Jian-yu Lu*

Ultrasound Laboratory, Department of Bioengineering, The University of Toledo, Toledo, OH 43606, U.S.A.
Email: jilu@eng.utoledo.edu

*Abstract* – Recently, a high frame rate (HFR) imaging method based on limited diffraction beam (LDB) theory has been developed. In this method, a two-dimensional (2D) or three-dimensional (3D) image is constructed with a single plane wave transmission and thus a theoretical frame rate of 3750 frames/second can be obtained for biological soft tissues at a depth of about 200 mm. Because a plane wave is used to transmit, images can only be obtained in a small area if an object is illuminated with a transducer of a small footprint. In this paper, we extend the HFR method by using a cylindrical wave to illuminate an object. Mathematical formulas were derived and computer simulations were performed to verify the method. The method allows to increase the illumination area by using a transducer of a small footprint, which is important for applications such as cardiac imaging where acoustic window sizes are limited.

## I. INTRODUCTION

Traditionally, medical ultrasound images are obtained with focused beams that illuminate only a small area. To construct an image, multiple transmissions of ultrasound beams are required. Because the speed of sound in biological soft tissues is finite (about 1500 m/s), image frame rate is low, leading to distorted images of fast moving objects such as the heart and flowing blood. To increase frame rate, the number of transmissions needs to be reduced. Recently, a high frame rate (HFR) imaging method has been developed based on limited diffraction beam (LDB) theory [1,2]. With this method, a theoretical frame rate of 3750 frames/s can be achieved for either 2D or 3D imaging of biological soft tissues (speed of sound of about 1500 m/s) at a depth of about 200 mm. Although the frame rate is potentially high, this method requires a transducer of large footprint in order to illuminate an entire object of interest, which is not suitable for applications where acoustic windows are small and thus a small footprint is desirable.

In this paper, a cylindrical wave instead of a plane wave is used in transmission. This reduces the footprint while maintaining a high frame rate and increasing image field of view. To construct images, a relationship between the filtered object function such as ultrasound reflectivity distribution and received echo signals was developed. Because the filter has a very sharp spatial response (similar to a $\delta$ -function), high-resolution and low-sidelobe images can be constructed. To verify the method, computer simulations were performed. Results are consistent with those predicted by the theory.

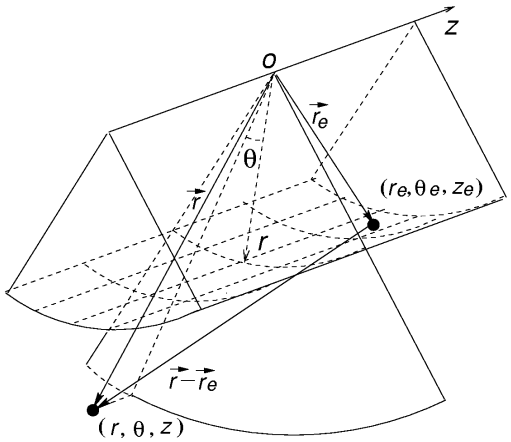


**Fig. 1.** Cylindrical coordinate of transducer and a point scatterer

## II. THEORY

In this section, a relationship between the filtered object function and the received echo signals will be developed. From the wave equation, it is clear that a cylindrical wave can be approximated with a zeroth-order Hankel function [3]. If the argument of the

Hankel function is much larger than 1, we have the following approximation:

$$p(r,k) \approx A(k)\frac{e^{ikr}}{\sqrt{kr}}, \tag{1}$$

where $k$ is the wave number, $r = \sqrt{x^2 + y^2}$ is the radial distance along the propagation direction of the cylindrical wave, and $A(k)$ is the transmission transfer function of the transducer.

From Eq. (1) and the Rayleigh-Sommerfeld diffraction formula [4], the temporal spectrum of the echo signal received from a transducer element at $(r_e, \theta_e, z_e)$ is given by (see Fig. 1 for the coordinate system):

$$\begin{aligned} R(k,\theta_e,z_e) &= \frac{\sqrt{k}}{i2\pi}A(k)T(k)\iiint_V drd\theta dz f(r,\theta,z) \\ &\times \frac{e^{ikr+ik\sqrt{r^2+r_e^2-2rr_e\cos(\theta_e-\theta)+(z_e-z)^2}}}{r^2+r_e^2-2rr_e\cos(\theta_e-\theta)+(z_e-z)^2} \\ &\times\sqrt{r}(r\cos(\theta_e-\theta)-r_e), \end{aligned} \tag{2}$$

where $\theta$ is polar angle, $r$ is the radius, $z$ is the axis of the cylinder, which is perpendicular to the plane defined by $r$ and $\theta$, and $V$ is the volume of object. $T(k)$ is the reception transfer function of the transducer, and $f(r,\theta,z)$ is the object function, where $(r,\theta,z)$ represents the coordinate of a point scatter.

Our objective is to construct the object function from (2). It is clear that (2) is a convolution of the functions $f(r,\theta,z)$ and $h(k,r,\theta,z)$ in terms of both $\theta$ and $z$, i.e.,

$$R(k,\theta_e,z_e) = \int_{r_e}^{\infty} drf(r,\theta,z) *_{\theta,z} h(k,r,\theta,z), \tag{3}$$

where $*_{\theta,z}$ represents the convolution in terms of both $\theta$ and $z$, and $h(k,r,\theta,z)$ is defined as:

$$\begin{aligned} h(k,r,\theta,z) &= \frac{\sqrt{k}}{i2\pi}A(k)T(k) \\ &\times \frac{e^{ikr+ik\sqrt{r^2+r_e^2-2rr_e\cos\theta+z^2}}}{r^2+r_e^2-2rr_e\cos\theta+z^2}\sqrt{r}(r\cos\theta-r_e), \end{aligned} \tag{4}$$

Taking Fourier transform on both sides of (3), we have:

$$\begin{aligned} \tilde{R}(k,k_\theta,k_z) &= \mathcal{F}_{\theta,z}\{R(k,\theta,z)\} \\ &= \int_{r_e}^{\infty} dr\tilde{F}(r,k_\theta,k_z)\tilde{H}(k,r,k_\theta,k_z), \end{aligned} \tag{5}$$

where $\tilde{R}(k,k_\theta,k_z)$ and $\tilde{H}(k,r,k_\theta,k_z)$ are the Fourier transform of $R(k,\theta,z)$ and $h(k,r,\theta,z)$, respectively, in terms of both $\theta$ and $z$.

Multiplying both sides of (5) with $\tilde{H}^*(k,r',k_\theta,k_z)$, where "$*$" represents complex conjugation, and then integrating the results over the wave number, $k$, we have:

$$\begin{aligned} \tilde{R}'(r',k_\theta,k_z) &= \int_{-\infty}^{\infty} dk\tilde{R}(k,k_\theta,k_z)\tilde{H}^*(k,r',k_\theta,k_z) \\ &= \int_{r_e}^{\infty} dr\tilde{F}(r,k_\theta,k_z)G(r,r',k_\theta,k_z), \end{aligned} \tag{6}$$

where

$$G(r,r',k_\theta,k_z) = \int_{-\infty}^{\infty} dk\tilde{H}(k,r,k_\theta,k_z)\tilde{H}^*(k,r',k_\theta,k_z). \tag{7}$$

It is clear from (6) that the point spread function (PSF) of the imaging system is given by: $g(r,r',\theta,z) = \mathcal{F}^{-1}_{k_\theta,k_z}\{G(r,r',k_\theta,k_z)\}$. From Fig. 2, one can see that the PSF has a sharp peak around $r = r'$, $\theta = 0$, and $z = 0$, and thus the following relationship can be assumed:

$$|g(r,r',\theta,z)| \approx |g'(r-r',\theta,z)|. \tag{8}$$

From (6) and (8), the object function can be constructed approximately:

$$f'(r,\theta,z) \approx \mathcal{F}^{-1}_{k_\theta,k_z}\{\tilde{R}'(r,k_\theta,k_z)\}$$
$$\approx f(r,\theta,z) *_{r,\theta,z} g'(r,\theta,z) \approx f(r,\theta,z), \quad (9)$$

where $*_{r,\theta,z}$ represents the convolution with respect to $r,\theta$, and $z$. For an ideal imaging system where $g'(r,\theta,z)$ is a $\delta$-function, $f'(r,\theta,z)$ is the object function, $f(r,\theta,z)$.

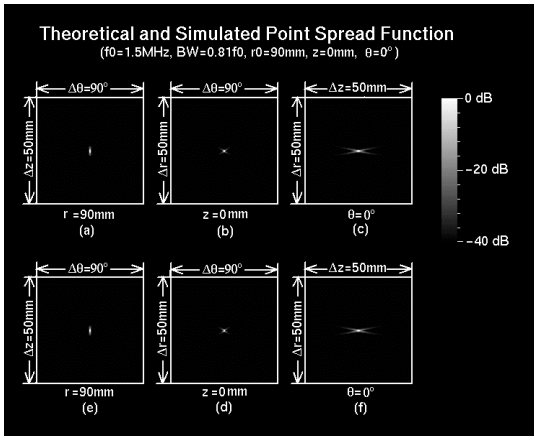


**Fig. 2**. Theoretical (top row) and constructed (bottom row) point spread functions (PSF) of the cylindrical wave imaging system in $z-\theta$ ((a) and (d)), $r-\theta$ ((b) and (e)), and $r-z$ ((c) and (f)) planes.

## III. SIMULATION

To verify the theory developed in the previous section, computer simulations were performed. In the simulation, the following parameters were assumed: the transducer had a center frequency of 1.5 MHz, the combined transmission and reception transfer function, $A(k)T(k)$, was represented with a Blackman window function with a full width at half maximum (FWHM) or –6dB bandwidth of about 81% of the center frequency, the speed of sound of the medium was 1500 m/s, the radius of the cylindrical transducer, $r_e$, was 40 mm; the width of the transducer in the $z$ direction was 50 mm, the angular width of the transducer was 90°, the number of elements of the transducer was $128\times128$ (along $z$ and $\theta$ directions), and objects were composed of point scatterers. In transmission, all the array elements were excited simultaneously to produce a cylindrical wave, which was obtained with the Rayleigh-Sommerfeld diffraction formula. Echoes from the object were received with the same array and processed to construct images with the theoretical analysis in the previous section. I.e., the steps below were followed:

1) Simulating the transmission wave with the Rayleigh-Sommerfeld diffraction formula.
2) Obtaining Fourier transform of received signal (see (5)) in terms of both $\theta$ and $z$ : $\tilde{R}(k,k_\theta,k_z) = \mathcal{F}_{\theta,z}\{R(k,\theta,z)\}$.
3) Multiplying the result with a known function, $\tilde{H}^*(k,r',k_\theta,k_z)$, and then integrating it over $k$ (see (6)).
4) Constructing image with an inverse Fourier transform (see (9)).

Two objects were used in the simulations. One contains a single point scatterer (Fig. 1) and another has 9 point scatterers located at three perpendicular planes (Fig. 3). The center of the objects is located at $(r_0,0,0)$. Constructed images of these objects are shown in Figs. 2 and 4, respectively.

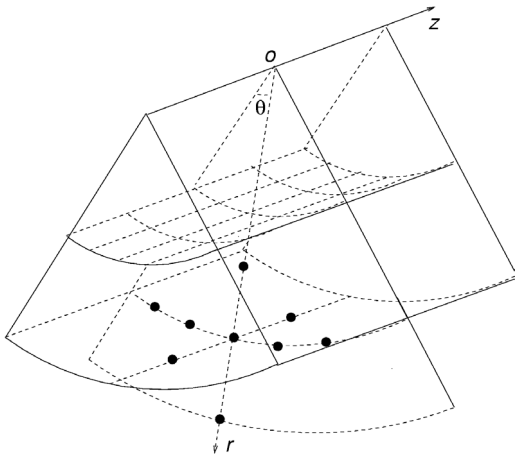


**Fig. 3.** A 3D object consisting 9 point scatterers in three orthogonal planes.

Figs. 2(a), 2(b), and 2(c) show the calculated PSF, $|g'(r-r',\theta,z)|$ (see (8)), in $z-\theta$ ($r=r'$ = 90 mm),

$r-\theta$ ($z$ = 0 mm and $r'$ = 90 mm), and $z-r$ ($\theta$ = 0° and $r'$ = 90 mm) planes, respectively. The PSF constructed from the received echo signal is shown in Figs. 2(d), 2(e), and 2(f), corresponding to Figs. 2(a), 2(b), and 2(c), respectively. The dimensions of the images are 50 mm in both $r$ and $z$ directions, and are 90° in $\theta$ direction. The distance of the point scatterer from the curvature center of the transducer is 90 mm. From Fig. 2, it is clear that the constructed PSF is very close to that calculated theoretically (see (7)).

Constructed images of the 3D object in Fig. 3 are shown in Fig.4. The distance between the centers of the 3D object and the transducer curvature is 90, 140, and 240 mm, respectively.

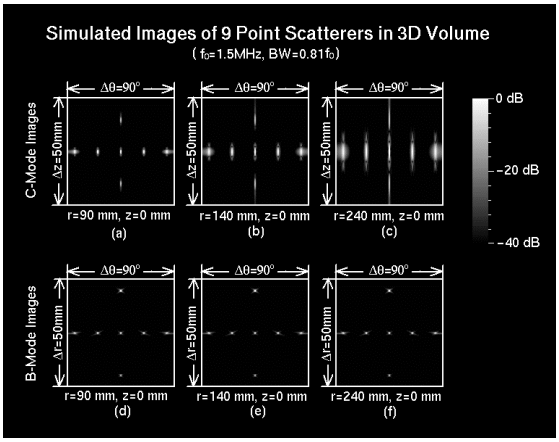


**Fig. 4.** Constructed images in $z-\theta$ (top row) and $r-\theta$ (bottom row) planes, at distances (between the centers of the 9-point object and the curvature of the cylindrical transducer) of 90 mm ((a) and (d)), 140 mm ((b) and (e)), and 240 mm ((c) and (f)).

## IV. CONCLUSION

A method has been developed to construct 3D images of an imaging system that uses a cylindrical wave in transmission. Because cylindrical wave is used, images of a larger field of view for a larger object can be constructed with a transducer of a smaller footprint. In addition, the method uses Fourier transform to construct images and thus the amount of computation required is smaller than that of the conventional delay-and-sum method.

Because only one transmission is needed to construct a 3D image, theoretically, image frame rate could be very high (up to 3750 frames/s for biological soft tissues at a depth of about 200 mm) with this method.

From computer simulations, it is seen that images of high resolution and low sidelobe can be constructed. In addition, the method can be easily adapted for 2D imaging where a 1D, instead of 2D array transducer is used. (In 2D case, object is assumed to be uniform along $z$ direction.) To compensate for signal-to-noise ratio due to diverging transmitting wave, coded excitations such as FM chirps can be used.

## V. ACKNOWLEDGEMENTS

This work was supported in part by the grant HL60301 from the National Institutes of Health (NIH).

## VI. REFERENCES

[1] Jian-yu Lu, "2D and 3D high frame rate imaging with limited diffraction beams," *IEEE Transactions on Ultrasonics, Ferroelectrics, and Frequency Control,* vol. 44, no. 4, pp. 839-856, July, 1997.

[2] Jian-yu Lu, "Experimental study of high frame rate imaging with limited diffraction beams," *IEEE Transactions on Ultrasonics, Ferroelectrics, and Frequency Control,* vol. 45, no. 1, pp. 84-97, January, 1998.

[3] P. M. Morse and H. Feshbach, *Methods of Theoretical Physics,* Part I, New York: McGraw-Hill, 1953.

[4] J. W. Goodman, *Introduction to Fourier Optics,* McGraw-Hill, New York, 1968.